Endochronic prediction for the mechanical ratchetting of a stepped beam subjected to steady tension and cyclic bending

W.F. Pan † and Y.S. Yang

*Department of Engineering Science, National Cheng Kung University,
Tainan, Taiwan, 70101, R.O.C*

J.K. Lu

*Department of Civil Engineering, National Pingtung Polytechnic Institute,
Pingtung, Taiwan, 91207, R.O.C.*

Abstract. In this paper, the first-order ordinary differential constitutive equations of endochronic theory are incorporated into finite element formalism. A theoretical investigation is performed on the ratchetting effect of a stepped beam subjected to steady tension and cyclic bending. Experimental data of lead alloy found in literature are used for comparison. Those data reveal that the endochronic prediction yields more adequate results than those predictions using the plasticity models with isotropic hardening or kinematic hardening, as employed by Hardy, *et al.* (1985).

Key words: endochronic theory; finite element formulism; stepped beam; cyclic bending.

1. Introduction

More thoroughly understanding the behavior of material ratchetting is essential in designing mechanical or structural systems such as a power plant or components of nuclear reactors. Some simple models incorporated with finite element method to analyze the complex geometry components with complex loading conditions yield poor predictions of the material behavior when compared with experimental findings. As is generally known, the prediction accuracy for real engineering problems depends on the modelling of the components, the component materials, and loading conditions. Owing to the rapid progress in computer technology, some realistic and complex models can be implemented to satisfy an increasing demand to accurately simulate the response of real materials.

Endochronic theory, as originally proposed by Valanis (1971), is a different approach to describe elasto-plastic behavior of history-dependent materials. The theory is based upon irreversible thermodynamics and employs the concept of internal variables. The key concept of the theory is the intrinsic time which is originally defined in terms of a total strain tensor (Valanis 1971). Moreover, the theory was developed without any concept of yield surface. The

---

† Associate Professor

definition of the intrinsic time has led to difficulties in cases where the history of deformation involves unloading. This was subsequently modified by reformulating the intrinsic time in terms of the plastic strain tensor (Valanis 1980). After its introduction, the theory has been successfully applied in describing material responses, such as metals (Wu and Yip 1981, Valanis and Fan 1983, Valanis and Lee 1984, Watanabe and Atluri, 1985, Fan and Peng 1991), soils (Wu and Aboutorabi 1988, Imai and Xie 1990), concretes (Bazant and Bhat 1976, Valanis and Read 1986), composites (Mathison, *et al.* 1991), and porous materials (Wu, *et al.* 1990). The kernel function of the theory exhibits the weak singularity at the zero intrinsic time and is integrable in a finite domain. According to the mathematical characteristics, Murakami and Read (1989) used a group of exponential decaying functions to form the kernel function. Thus, the constitutive equations of the theory could then be simplified into first-order ordinary differential constitutive equations. Moreover, they also investigated the performance of these equations with and without Richardson extrapolation. It was shown that the extrapolation methods provide a significant increase in computational speed for comparable accuracy.

Hyde, *et al.* (1985) conducted the first experiments involving a beam component of a lead alloy subjected to steady tension and cyclic bending in an attempt to investigate the ratchetting effect of a material. The accumulation of the strain amplitude on the top and bottom surfaces was measured. The model, as proposed by Goodman and Goodall (1981), was incorporated into the finite element program for simulating the beam component's ratchetting behavior. Fessler and Hyde (1985) tested stepped beam components made of the same material under steady tension and cyclic bending. Fig. 1 shows the geometry and dimensions of the stepped beam component. The prismatic part (shank) is loaded in an axial direction, but there is a stress concentration and non-uniaxial stress state in the region of the fillet (circular arc). Strains were measured in the fillets at the step as well as in the shank of the stepped beam component. They discovered that the ratchetting strains per cycle decreased during each cycle, and the steady state values were related to the load magnitudes. Later, Hardy, *et al.* (1985) made predictions of experimental results tested by Fessler and Hyde (1985). In their study, the creep effect caused by the steady tension was neglected owing to the short duration time. In addition, the elastic-perfectly plastic model and the classical plasticity model with isotropic hardening or kinematic hardening were incorporated into finite element programs to describe the stepped beam's ratchetting behavior. Their results depicted that none of those models provide accurate predictions for the beam's ratchetting behavior.

In this paper, we incorporate the first-order ordinary differential constitutive equations into the finite element formalism for the sake of simulating the material ratchetting behavior of a stepped beam subjected to steady axial load and cyclic bending. Experimental data tested by Hyde, *et al.* (1985) are used to compare with the endochronic simulation. A better approximation for the uniaxial cyclic stress-strain curve and the cyclic strain-moment curves for the top and bottom of the beam's surface is obtained when compared with the simulation used by Hyde, *et al.* (1985). Moreover, experimental data tested by Fessler and Hyde (1985) are also compared with the endochronic simulation. The strain variations in the shank and fillet areas for the top and bottom of the surface of the beam are calculated. This study also included theoretical predictions according to classical plasticity models with isotropic hardening or kinematic hardening employed by Hardy, *et al.* (1985). Those results indicated that owing to the accurate description of the material's elastic-plastic behavior, the endochronic model provides a more accurate prediction of the material ratchetting behavior than the predictions of the two models employed the Hardy, *et al.* (1985).

2. Endochronic theory for elasto-plastic deformation

Under the condition of small deformation, the endochronic constitutive equations are expressed as follows (Valanis 1980):

$$\underset{\sim}{s} = 2 \int_0^z \rho(z-z') \; \frac{\partial \underset{\sim}{e}^p}{\partial z'} dz'$$

(1)

and

$$d\underset{\sim}{e}^p = d\underset{\sim}{e} - \frac{d\underset{\sim}{s}}{2\,\mu_0}$$

(2)

in which $\underset{\sim}{s}$ and $\underset{\sim}{e}$ denote the deviatoric stress and strain tensors, respectively, $\underset{\sim}{e}^p$ is the deviatoric plastic strain tensor, μ_0 is the elastic shear modulus, $\rho(z)$ is the kernel function, and z is the intrinsic time scale. The intrinsic time measure ζ is defined to be

$$d\,\zeta = \parallel d\underset{\sim}{e}^p \parallel$$

(3)

where $\parallel \cdot \parallel$ is the Euclidean norm. The relationship between intrinsic time scale and measure is

$$\frac{d\,\zeta}{dz} = 1 - C\,e^{-\beta\zeta}, \quad C < 1$$

(4)

where C and β are material parameters. If the material is assumed to be plastically incompressible, it can be expressed as

$$d\,\sigma_{kk} = 3\,K\,d\,\varepsilon_{kk}$$

(5)

in which K is the elastic bulk modulus.

The kernel function $\rho(z)$ is a weakly singular function at the origin and integrable in the domain $0 \leq z \leq \infty$ (Valanis 1980), i.e.,

$$\rho(0) = \infty$$

(6)

and

$$\int_0^z \rho(z')\,dz' < \infty, \quad 0 < z < \infty.$$

(7)

Based on the above mathematical characteristics, $\rho(z)$ can be approximated by a finite sum of decaying exponential functions (Murakami and Read 1989), i.e.,

$$\rho(z) \cong \sum_{r=1}^{n} C_r e^{-\alpha_r z} \;\; ; \;\; \rho(0) = \sum_{r=1}^{n} C_r = \text{large number}$$

(8a, b)

where C_r and α are material parameters. By considering the kernel function in Eq. 8(a) and by using the Leibniz's differential rule, one obtains

$$\underset{\sim}{s} = \sum_{r=1}^{n} \underset{\sim}{s}_r$$

(9)

and

$$\frac{d\underset{\sim}{s}_r}{dz} + \alpha_r \underset{\sim}{s}_r = C_r \frac{d\underset{\sim}{e}^p}{dz}.$$

(10)

From Eqs. (9) and (10), the deviatoric stress increment is determined to be

$$d\underset{\sim}{s} = \sum_{r=1}^{n} d\underset{\sim}{s}_r = 2 \sum_{r=1}^{n} C_r \, d\underset{\sim}{e}^p - \sum_{r=1}^{n} \alpha_r \underset{\sim}{s}_r \, dz.$$

(11)

By considering the total stress $\underset{\sim}{\sigma}$ and the total strain tensor $\underset{\sim}{\varepsilon}$, Eq. (11) becomes

$$d\underset{\sim}{\sigma} = \sum_{r=1}^{n} d\underset{\sim}{\sigma}_r = p_1 \, d\underset{\sim}{\varepsilon} + p_2 \, d\varepsilon_{kk} \underset{\sim}{I} + p_3 \sum_{r=1}^{n} \alpha_r \left(\underset{\sim}{\sigma} - \frac{\sigma_{kk}}{3} \underset{\sim}{I} \right)_r dz$$

(12)

and

$$p_1 = \frac{2\mu_0 \sum\limits_{r=1}^{n} C_r}{\mu_0 + \sum\limits_{r=1}^{n} C_r}, \quad p_2 = K - \frac{1}{3}p_1, \quad p_3 = \frac{-p_1}{2\sum\limits_{r=1}^{n} C_r}$$

(13a, b, c)

in which $\underset{\sim}{I}$ is the unit tensor.

3. Endochronic formulation on the finite element method for plane stress state

The endochronic constitutive equations for general loading condition are expressed from Eq. (12) to be

$$\{d\sigma\} = [D]\{d\varepsilon\} + p_3\{H\}dz$$

$$\begin{Bmatrix} d\sigma_{xx} \\ d\sigma_{yy} \\ d\sigma_{zz} \\ d\sigma_{xy} \\ d\sigma_{yz} \\ d\sigma_{zx} \end{Bmatrix} = \begin{bmatrix} p_1+p_2 & p_2 & p_2 & 0 & 0 & 0 \\ p_2 & p_1+p_2 & p_2 & 0 & 0 & 0 \\ p_2 & p_2 & p_1+p_2 & 0 & 0 & 0 \\ 0 & 0 & 0 & \dfrac{p_1}{2} & 0 & 0 \\ 0 & 0 & 0 & 0 & \dfrac{p_1}{2} & 0 \\ 0 & 0 & 0 & 0 & 0 & \dfrac{p_1}{2} \end{bmatrix} \begin{Bmatrix} d\varepsilon_{xx} \\ d\varepsilon_{yy} \\ d\varepsilon_{zz} \\ 2d\varepsilon_{xy} \\ 2d\varepsilon_{yz} \\ 2d\varepsilon_{zx} \end{Bmatrix} + p_3 \begin{Bmatrix} H_{xx} \\ H_{yy} \\ H_{zz} \\ H_{xy} \\ H_{yz} \\ H_{zx} \end{Bmatrix} dz$$

(14)

where

$$H_{ij} = \sum_{r=1}^{n} \alpha_r (S_{ij})_r \qquad (i, \ j = x, \ y, \ z).$$

(15)

Each stress component is expressed as

$$d\sigma_{xx} = (p_1 + p_2)d\varepsilon_{xx} + p_2 d\varepsilon_{yy} + p_2 d\varepsilon_{zz} + p_3 H_{xx} dz$$
$$d\sigma_{yy} = p_2 d\varepsilon_{xx} + (p_1 + p_2)d\varepsilon_{yy} + p_2 d\varepsilon_{zz} + p_3 H_{yy} dz$$
$$d\sigma_{zz} = p_2 d\varepsilon_{xx} + p_2 d\varepsilon_{yy} + (p_1 + p_2)d\varepsilon_{zz} + p_3 H_{zz} dz$$
$$d\sigma_{xy} = p_1 d\varepsilon_{xy} + p_3 H_{xy} dz$$
$$d\sigma_{yz} = p_1 d\varepsilon_{yz} + p_3 H_{yz} dz$$
$$d\sigma_{zx} = p_1 d\varepsilon_{zx} + p_3 H_{zx} dz \qquad \text{(16a, b, c, d, e, f)}$$

In the plane stress condition, the values of $d\sigma_{zz}$, $d\sigma_{yz}$, $d\sigma_{zx}$ are equal to zero. Thus,

$$d\varepsilon_{zz} = \frac{-p_2 d\varepsilon_{xx} - p_2 d\varepsilon_{yy} - p_3 H_{zz} dz}{p_1 + p_2}$$

$$d\varepsilon_{yz} = \frac{-p_3 H_{yz} dz}{p_1}$$

$$d\varepsilon_{zx} = \frac{-p_3 H_{zx} dz}{p_1} \qquad \text{(17a, b, c)}$$

Substitution of Eqs. (17a), 17(b) and 17(c) into Eqs. (16a), (16b) and (16c) leads to

$$d\sigma_{xx} = \left(p_1 + p_2 - \frac{p_2^2}{p_1+p_2}\right)d\varepsilon_{xx} + \left(p_2 - \frac{p_2^2}{p_1+p_2}\right)d\varepsilon_{yy} + \left(p_3 H_{xx} - \frac{p_2 p_3}{p_1+p_2}H_{zz}\right)dz$$

$$d\sigma_{yy} = \left(p_2 - \frac{p_2^2}{p_1+p_2}\right)d\varepsilon_{xx} + \left(p_1 + p_2 - \frac{p_2^2}{p_1+p_2}\right)d\varepsilon_{yy} + \left(p_3 H_{yy} - \frac{p_2 p_3}{p_1+p_2}H_{zz}\right)dz$$

$$d\sigma_{xy} = p_1 d\varepsilon_{xy} + p_3 H_{xy} dz. \qquad \text{(18a, b, c)}$$

The endochronic constitutive equations can be expressed in terms of matrix notation as

$$\{d\sigma\} = [D]\{d\varepsilon\} + p_3\{H\}dz$$

$$\begin{Bmatrix} d\sigma_{xx} \\ d\sigma_{yy} \\ d\sigma_{xy} \end{Bmatrix} = \begin{bmatrix} p_1 + p_2 - \dfrac{p_2^2}{p_1+p_2} & p_2 - \dfrac{p_2^2}{p_1+p_2} & 0 \\[2mm] p_2 - \dfrac{p_2^2}{p_1+p_2} & p_1 + p_2 - \dfrac{p_2^2}{p_1+p_2} & 0 \\[2mm] 0 & 0 & \dfrac{p_1}{2} \end{bmatrix} \begin{Bmatrix} d\varepsilon_{xx} \\ d\varepsilon_{yy} \\ 2d\varepsilon_{xy} \end{Bmatrix}$$

$$+ p_3 \begin{Bmatrix} H_{xx} - \dfrac{p_2}{p_1+p_2}H_{zz} \\[2mm] H_{yy} - \dfrac{p_2}{p_1+p_2}H_{zz} \\[2mm] H_{xy} \end{Bmatrix} dz. \qquad \text{(19)}$$

By using Eq. (19) and the principle of virtual work, an initial stress finite element computational algorithm of the endochronic theory can be formulated. The governing equation is

$$(\int_v [B]^T [D][B]dV)\{da\} = -p_3(\int_v [B]^T dV)\{H\}dz + \int_v [N]^T \{dP\}dV + \int_S [N]^T\{dT\}dS \quad (20)$$

where $[B]$ is the strain-displacement matrix, $\{da\}$ is the displacement vector, $[N]$ is the shape function matrix, $\{dP\}$ is the body force vector, and $\{dT\}$ is the traction force vector. Eq. (20) can be rewritten as

$$[K]\{da\} = \{dF_p\}+\{dF_{ext}\} \quad (21)$$

and

$$[K] = \int_v [B]^T [D][B]dV$$

$$\{dF_p\} = -p_3(\int_v [B]^T dV)\{H\}dz$$

$$\{dF_{ext}\} = \int_v [N]^T \{dP\}dV + \int_S [N]^T \{dT\}dS \quad (22a, b, c)$$

where $[K]$ is called the stiffness matrix, $\{dF_p\}$ is the plastic pseudoforce, and $\{dF_{ext}\}$ is the external force.

The incremental elastoplastic solution is determined by iteratively revising the system of finite element equations by adding a vector of plastic pseudoforce. The nonlinear solution is then calculated by the solution of a series of linear equations and by varying the plastic pseudoforce. Once the difference between the calculated values of dz in Eq. (19) and Eq. (21) is less than some defined tolerance, a new loading or unloading process is then initiated.

4. Comparison and discussion of the theoretical and experimental results

In this section, we compare theoretical results with experimental data obtained by Hyde, *et al.* (1985), and Fessler and Hyde (1985). Hyde, *et al.* (1985) tested the beam component of a lead alloy subjected to cyclic uniaxial loading. Meanwhile, They also conducted an experiment on the beam component under steady axial tension and cyclic bending. Strains were measured at the top and bottom surfaces of the beams using electrical resistance strain gages. Theoretically, they used the plasticity model proposed by Goodman and Goodall (1981) and incorporated it into a finite element program for simulating the beam component's ratchetting behavior. Fessler and Hyde (1985) tested a stepped beam made of the same material subjected to steady tension and cyclic bending. Strains were measured in the fillets at the step and in the shank of the beam component. The geometry and dimensions of the stepped beam component is depicted in Fig. 1. In this study, we also include the theoretical predictions obtained by using classical plasticity theories with isotropic hardening (denoted as *IH*) or kinematic hardening (denoted as *KH*), which were employed by Hardy, *et al.* (1985).

Fig. 2 displays the finite element mesh used to model one half of the stepped beam component. The elements are 8-noded, plane stress, isoparametric elements. Fig. 3 shows the experimental stress-strain curve under a uniaxial cyclic strain-controlled test. Based on the experimental data in Fig. 3, the material parameters for the theory are determined according to the method proposed by Fan (1983) to be: $\mu_0=8.7\times 10^3$ MPa, $K=22.7\times 10^3$ MPa, $C=-0.08$, $\beta=70.0$, $C_1=2.65\times 10^4$ MPa, $\alpha_1=4.5\times 10^3$, $C_2=7.85\times 10^2$ MPa, $\alpha_2=4.5\times 10^2$, $C_3=2.8\times 10^2$ MPa and $\alpha_3=9.5\times 10^1$. The corresponding simulated result is also demonstrated in Fig. 3. According to this figure, the alloy exhibits the property of cyclic softening for uniaxial cyclic loading; therefore,

the material parameter C is found to be a negative value. Figs. 4 and 5 present the strain-moment curves at the first tensile (FT) surface (for z/d=0.48) and first compressive (FC) surface (for z/d=-0.48) at the shank area of the beams during the first complete cycle, respectively, where z is the distance from beam centre-line, d is beam depth, and M_y is the maximum elastic moment, which is equal to 22.34 N·m. It is shown that the endochronic simulation yields a better prediction than the model employed by Hyde, et al. (1985).

Next, the ratchetting effect of stepped beam component subjected to steady axial tension and cyclic bending is discussed in the following. The loading condition is ±23 N·m for the magnitude of the cyclic moment and 5.38 kN for the magnitude of the axial tension. Figs. 6 and 7 depict the calculated results of the stress-strain history of the beam component during fifteen cycles on the FT and FC surfaces as the shank of the beam, respectively. The ratchetting effect of the stress-strain behavior is observed, which is accompanied by a reduction in the width of the stress-strain loop when the number of cycles is increased. Figs. 8. and 9 present the variation of the strains on the FT and FC surfaces at the shank of the stepped beam with each of moment during the first three cycles, respectively. Due to the reversal of the moment produced con-
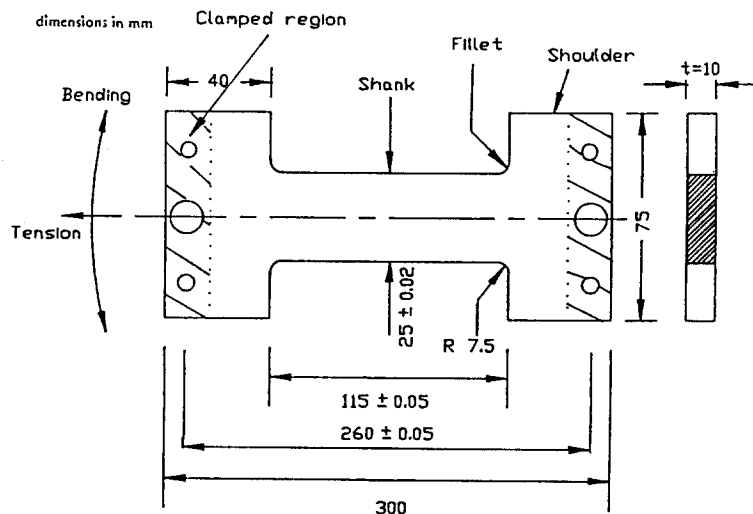
Fig. 1 The stepped beam component. Dimensions in mm.
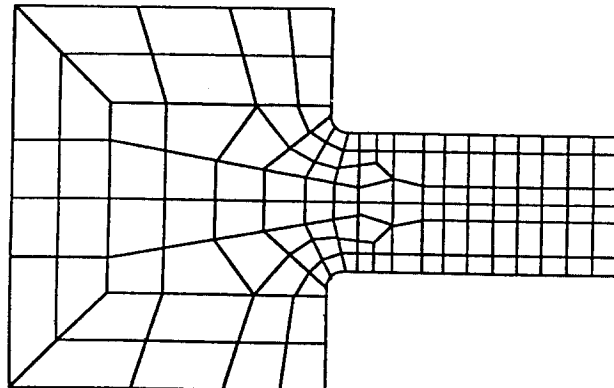

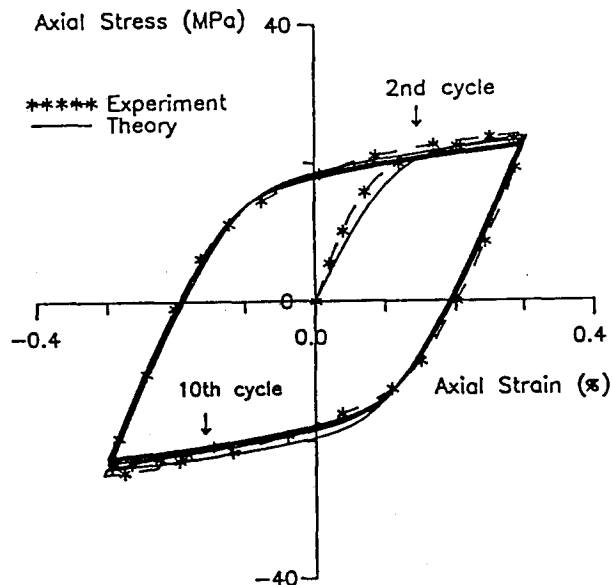Fig. 2 The finite element mesh.

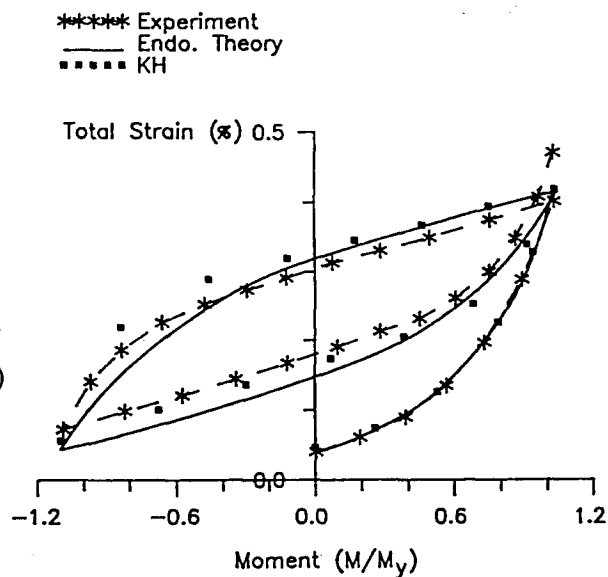Fig. 3 Uniaxial stress-strain curves under cyclic strain-controlled test.

Fig. 4 Variation of strain with moment for the shank at the *FT* surface.

siderable reverse plastic strain at the outer surface, the reverse strains are accompanied by a relatively small increment of strain in each cycle. Those figures indicate that the endochronic model yields a better prediction with the experimental data than the other·two models. Fig. 10 shows the theoretical and experimental results of the total accumulated strain vs. number of cycles on the *FT* and *FC* surfaces at the shank. Also, Fig. 11 exhibits the corresponding ratchet strain vs. number of cycles on the *FT* and *FC* surfaces at the shank. It is seen that the ratchet strains initially reduce rapidly with the cycle number from the first cycle value. After the first two or three cycles, the rate of reduction is relatively small. Figs. 12 and 13 present the vari-
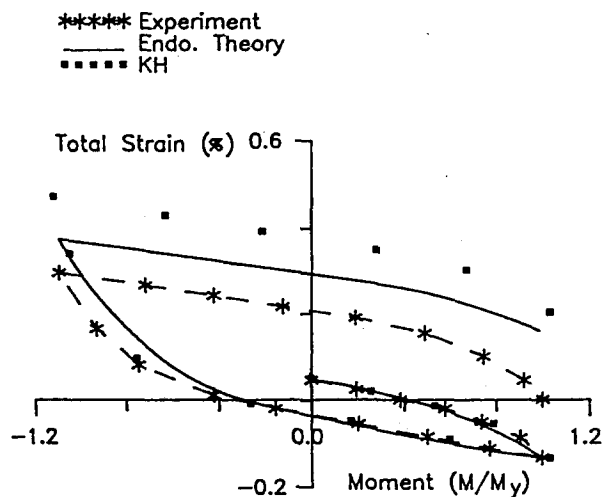
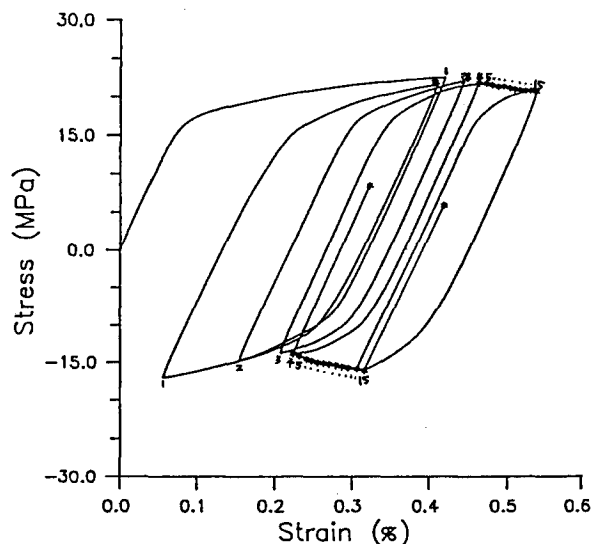Fig. 5 Variation of strain with moment for the shank at the *FC* surface.

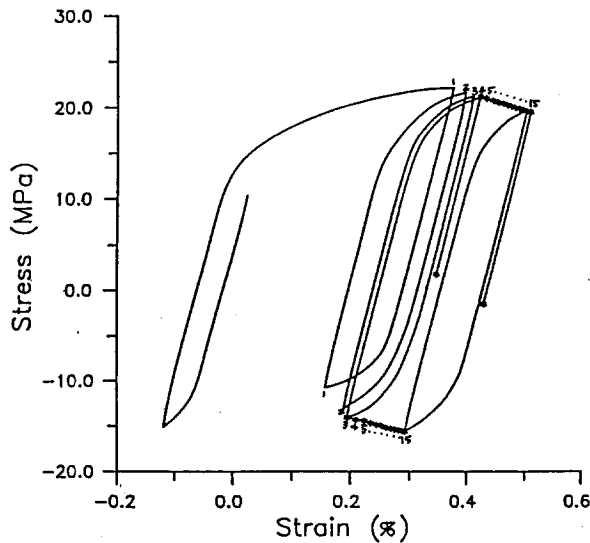Fig. 6 Theoretical stress-strain curves for the shank at the *FT* surface.

Fig. 7 Theoretical stress-strain curves for the shank at the *FC* surface.
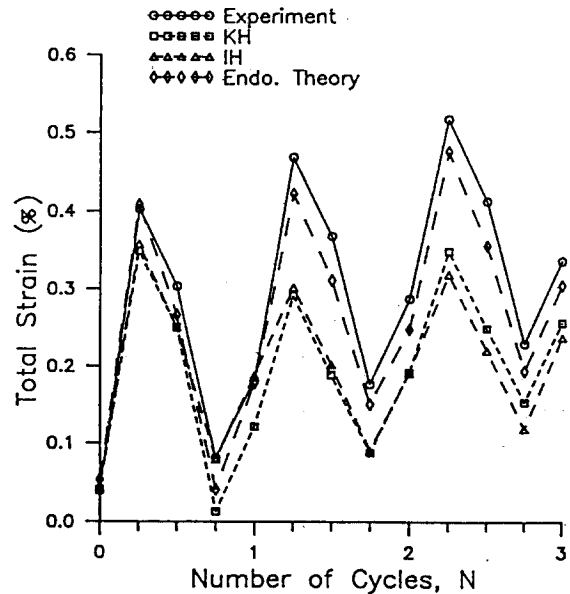

Fig. 8 Variation of strain with number of cycles for the shank at the *FT* surfaces.

ation of the strains on the *FT* and *FC* surfaces at the fillet of the stepped beam with each of moment for ten moment cycles, respectively. According to those figures, the accumulated total strains rapidly increase with the progress round the fillet towards the shank; the locations of the maximum strain are very close to the fillet-shank transitions. A comparison with the experimental data reveals that the endochronic theory incorporated into the finite element formulism in simulating behavior the beam element yields the most satisfactory result.
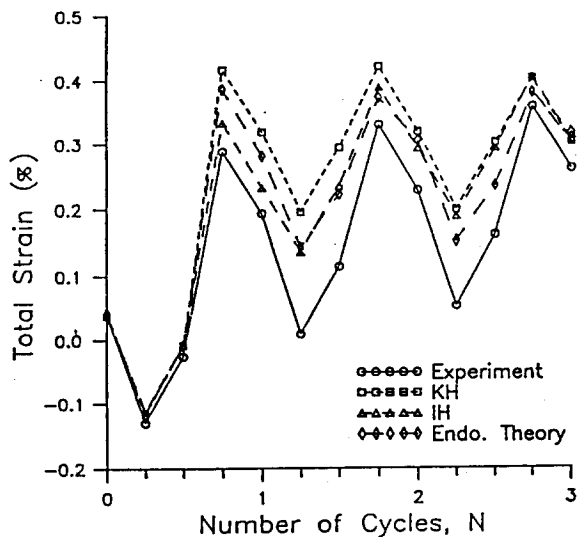

Fig. 9 Variation of strain with number of cycles for the shank at the *FC* surface.
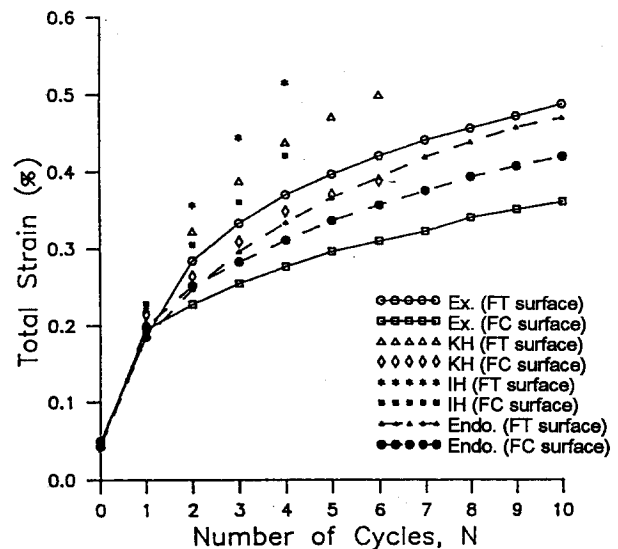

Fig. 10 Total accumulated strain vs. number of cycles for the shank at the *FT* and *FC* surfaces.
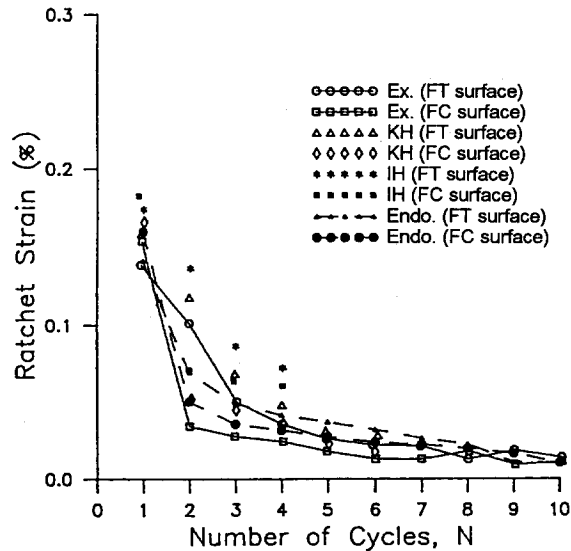
Fig. 11 Ratchet strain vs. number of cycles for the shank at the *FT* and *FC* surfaces.
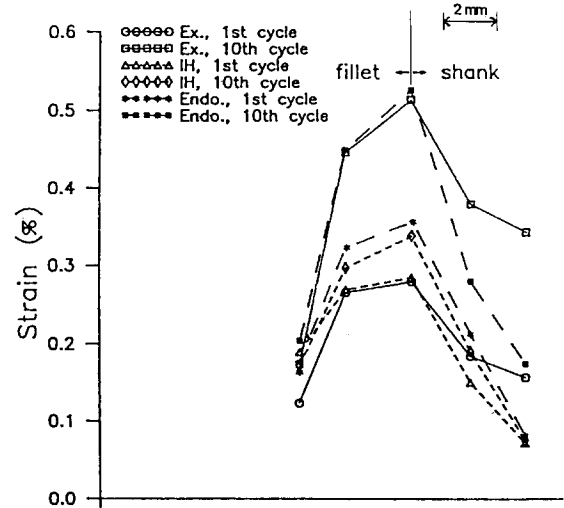

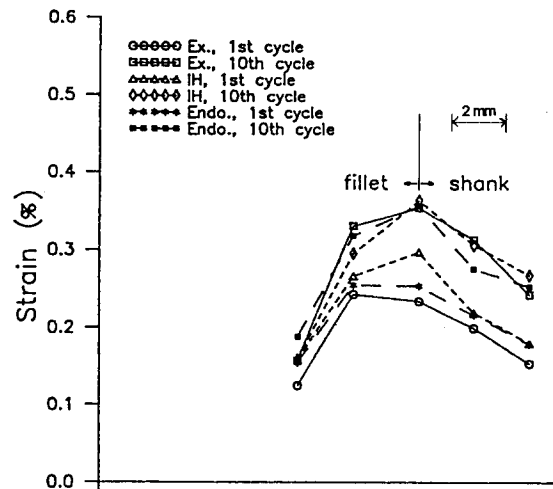Fig. 12 Variation of strain for the filet at the *FT* surface.

Fig. 13 Variation of strain for the fillet at the *FC* surface.

5. Conclusions

In this paper, we incorporate the first-order differential constitutive equations of endochronic theory derived by Murakami and Read (1989) into the finite element formalism. Theoretical investigations on the stepped beam components of a lead alloy subjected to steady tension and cyclic bending is made. The ratchetting effect in the (circular arc) fillets at the step and in the shank of the stepped beam component are studied. Experimental data tested by Hyde, *et al.* (1985) and Fessler and Hyde (1985) are used for comparison. In addition, theoretical predictions by using the plasticity models with isotropic or kinematic hardening, as employed by Hardy, *et al.* (1985), are also included for comparison. It is shown that the endochronic prediction yields more adequate results when compared with the experimental data and the predictions by two

plasticity models (Hardy, *et al.* 1985).

References

Bazant, Z.P. and Bhat, P.D. (1976), "Endochronic theory of inelasticity and failure for concrete", *J. Engng. Mech. Div., Proc. ASME,* **102**, EM4, 701-722.

Fan, J. (1983), "A comprehensive numerical study and experimental verification of endochronic plasticity", Ph. D. Dissertation, Department of Aerospace Engineering and Applied Mechanics, University of Cincinnati.

Fan J. and Peng X. (1991), "A physically based constitutive description for nonproportional cyclic plasticity", *J. Engng. Mater. Tech.,* **113**, 254-262.

Fessler, H. and Hyde, T.H. (1985), "Ratchetting tests of a stepped beam under steady tension and cycling bending", *J. Strain Analysis,* **20**(4), 193-200.

Goodman, A.M. and Goodall, I.W. (1981), "Constitutive relations for stainless steels", *Metals Society Conference.,* Varese.

Hardy, S.J., Webster, J.J. and Hyde, T.H. (1985), "An assessment of simple material behaviour models for predicting the mechanical ratchetting of a stepped beam", *J. Strain Analysis,* **20**(2), 63-78.

Hyde, T.H., Sahari, B.B. Sahari and Webster, J.J. (1985), "The effect of material ratchetting on the incremental growth of beams subjected to steady axial loads and cycle bending", *Int. J. Mech. Sci.,* **27**(4), 207-223.

Imai G. and Xie, C. (1990), "An endochronic constitutive law for static shear behavior of over-consolidated clays", *Soils and Foundations,* Japanese Society of Soil Mechanics and Foundation Engineering, **30**(1), 65-75.

Mathison, S.R., Pindera, M.J. and Herakovich C.T. (1991), "Nonlinear response of resin matrix laminates using endochronic theory", *J. Engng. Mater. Tech.,* **113**, 449-455.

Murakami, H. and Read, H.E. (1989), "A second-order numerical scheme for integrating the endochronic plasticity equations", *Computers and Structures,* **31**, 663-672.

Valanis, K.C. (1971), "A theory of viscoplasticity without a yield surface, Part I-general theory; Part II-application to mechanical behavior of metals", *Archive Mechanics,* **25**, 517-551.

Valanis, K.C. (1980), "Fundamental consequence of a new intrinsic time measure-plasticity as a limit of the endochronic theory", *Archive Mechanics,* **32**, 171-191.

Valanis, K.C. and Fan, J. (1983), "Endochronic analysis of cyclic elastoplastic strain fields in a notched plate", *J. Appl. Mech.* **50**, 789-794.

Valanis, K.C. and Lee, C.F. (1984), "Endochronic theory of cyclic plasticity with applications", *J. Appl. Mech.,* **51**, 367-374.

Valanis, K.C. and Read H.E. (1986), "An endochronic plasticity theory for concrete", *Mech. Mater.,* **5**, 277-295.

Watanabe, O. and Atluri, S.N. (1985), "A new endochronic approach to computational elasto-plasticity: and example of cyclically loaded cracked plate", *J. Appl. Mech.,* **52**, 857-864.

Wu, H.C. and Yip, M.C. (1981), "Endochronic description of cyclic hardening behavior for metallic material", *J. Engng. Mat. Tech.,* **103**, 212-217.

Wu, H.C. and Aboutorabi, M.R. (1988), "Endochronic model of sand with circular stress path", *J. Geotech. Engng.,* **114**(1), 95-105.

Wu, H.C., Wang, T.P., Pan, W.F. and Xu, Z.Y. (1990), "Cyclic stress-strain response of porous aluminum", *Int. J. Plasticity,* **6**, 207-230.